Biodegradable Polymer Blends of Poly(3-hydroxybutyrate) and Poly(DL-lactide)-*co*-poly(ethylene glycol)

LIANLAI ZHANG,[1,2] XIANMO DENG,[1] SHUJIE ZHAO,[3] ZHITANG HUANG[2]

[1] Chengdu Institute of Organic Chemistry, Academia Sinica, P.O. Box 415, Chengdu 610041, People's Republic of China

[2] Institute of Chemistry, Academia Sinica, Beijing 100080, People's Republic of China

[3] Chengdu Institute of Biology, Academia Sinica, Chengdu 610041, People's Republic of China

Received 23 July 1996; accepted 21 January 1997

ABSTRACT: The melting and crystallization behavior and phase morphology of poly(3-hydroxybutyrate)(PHB) and poly(DL-lactide)-*co*-poly(ethylene glycol)(PELA) blends were studied by DSC, SEM, and polarizing optical microscopy. The melting temperatures of PHB in the blends showed a slight shift, and the melting enthalpy of the blends decreased linearly with the increase of PELA content. The glass transition temperatures of PHB/PELA (60/40), (40/60), and (20/80) blends were found at about 30°C, close to that of the pure PELA component, during DSC heating runs for the original samples and samples after cooling from the melt at a rate of 20°C/min. After a DSC cooling run at a rate of 100°C/min, the blends showed glass transitions in the range of 10–30°C. Uniform distribution of two phases in the blends was observed by SEM. The crystallization of PHB in the blends from both the melt and the glassy state was affected by the PELA component. When crystallized from the melt during the DSC nonisothermal crystallization run at a rate of 20°C/min, the temperatures of crystallization decreased with the increase of PELA content. Compared with pure PHB, the cold crystallization peaks of PHB in the blends shifted to higher temperatures. Well-defined spherulites of PHB were found in both pure PHB and the blends with PHB content of 80 or 60%. The growth of spherulites of PHB in the blends was affected significantly by 60% PELA content. © 1997 John Wiley & Sons, Inc. J Appl Polym Sci **65:** 1849–1856, 1997

Key words: poly(3-hydroxybutyrate); poly(DL-lactide)-*co*-poly(ethylene glycol); blend; thermal behavior; morphology

INTRODUCTION

Poly(3-hydroxybutyrate)(PHB) is a thermoplastic polyester produced via biosynthesis by bacterial fermentation or transgenic plants. It can be degraded to water and carbon dioxide under environmental conditions by a variety of bacteria. PHB is representative of a useful range of potential biodegradable polymers.[1,2] However, the physical properties of PHB are not suitable for some biodegradable plastic and biomedical applications[3,4] because it shows some disadvantages, for example, brittleness, a narrow processability window, and a lower biodegradation rate than synthetic aliphatic polyesters. To improve its impact resistance and processability, a series of copolymers were biosynthesized by bacterial fermentation.[5] These copolymers were based on 3-hydroxybutyrate units and other hydroxyalka-

Correspondence to: L. Zhang, Department of Chemistry, National University of Singapore, Singapore 119260 (chmzll@leonis.nus.sg).

noate units such as poly(3-hydroxybutyrate-*co*-3-hydroxyvalerate) and poly(3-hydroxybutyrate-*co*-4-hydroxybutyrate) copolymers.

The development of biodegradable polymer blends with an optimum balance of physical properties and biodegradability is of key importance to relieve environmental problems concerning the disposal of nondegradable plastic materials. Many studies have focused on developing blends of bacterial polyester with poly(ethylene oxide),[6–10] poly(vinylene fluoride),[11,12] poly(vinyl acetate),[13] ethylene propylene rubber, ethylene–vinyl acetate copolymer,[13,14] polyepichlorohydrin,[15–17] poly(vinyl alcohol),[18,19] poly(vinyl phenol),[20] poly(methyl methacrylate),[9,21–23] and poly(cyclohexyl methacrylate).[21] But most of the second components used in PHB blends are nonbiodegradable, and thus the blends are not suited for biomedical application.

Synthetic aliphatic polyesters, another class of biodegradable polymers, such as polyglycolide, poly(L-lactide) (PLLA), poly(DL-lactide) (PDLLA), and poly(ϵ-caprolactone) (PCL), have found frequent applications as biodegradable matrices for prosthetics and controlled drug delivery. Naturally, blends containing PHB and synthetic aliphatic polyesters have been investigated to modify the physical properties, improve the processability, and adjust the biodegradation rate. PHB/PLLA,[24] PHB/PDLLA,[25] PHB/PCL,[26–27] and PHB/synthetic poly(3-hydroxybutyrate)[30–32] blends are well documented, so far. In our previous article blends of PHB and PDLLA, PCL, and poly(ester–ether) copolymers were preliminarily studied.[33] In this work, we investigate the melting and crystallization behavior and the phase morphology of PHB/poly(DL-lactide)-*co*-poly(ethylene glycol) (PELA) blends.

EXPERIMENTAL

Materials

PHB, obtained from Chengdu Institute of Biology, Academia Sinica, was prepared via bacterial fermentation, using methanol as a carbon source, by methylotrophic strain 8502-3 (*Hyphomicrobium zavarzinii* subsp. *chengduense* subsp. *nov.*).[34] The weight average molecular weight ($\bar{M}_w$) (3.0×10^5) was determined by intrinsic viscosity measurement in chloroform using the relationship $[\eta] = 1.18 \times 10^{-4} \bar{M}_w^{0.78}$ *at 30°C*.[35] PELA was synthesized by the ring-opening copolymerization of D,L-lactide and poly(ethylene glycol) (PEG, number average molecular weight 4000) with Al(*i*-Bu)$_3$—H_2O—H_3PO_4 complex catalyst.[36] The resultant copolymers contained 8 wt % PEG determined by ^{1}H-NMR. The weight average molecular weight was 3.6×10^4; this measurement was by gel permeation chromatography with THF as solvent.

Preparation of Blends

Thin films of PHB/PELA blends (weight ratios of 100/0, 80/20, 60/40, 40/60, 20/80, and 0/100) were prepared by casting from a 3% (w/v) solution of the two components in chloroform. The solvent was allowed to evaporate at room temperature overnight; then it was kept at 40°C under a vacuum for 48 h.

Differential Scanning Calorimetry (DSC)

DSC analysis was performed to study the miscibility and thermal behavior of the blends. A Perkin–Elmer DSC 7 apparatus equipped with a PE 3700 data station was utilized. The apparatus, calibrated with an indium standard in a nitrogen atmosphere, was used throughout.

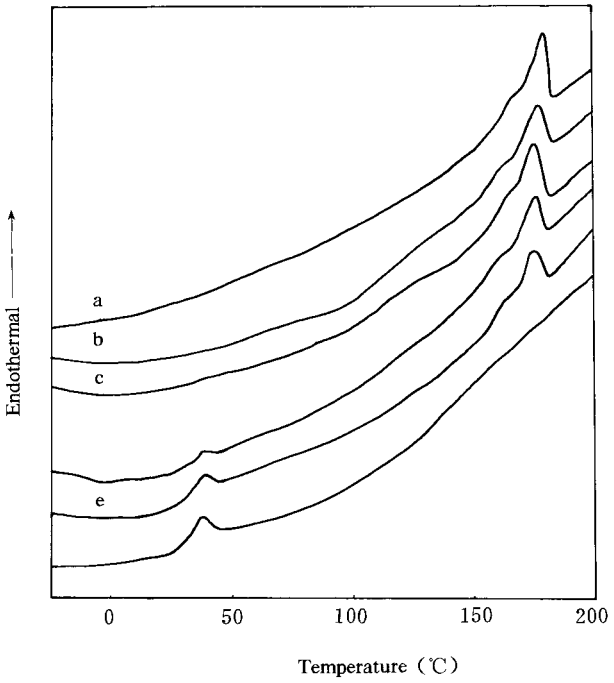

Figure 1 Differential scanning calorimetry thermograms of original samples during a heating run at a rate of 20°C/min: (a) PHB; (b) PHB/PELA (80/20); (c) PHB/PELA (60/40); (d) PHB/PELA (40/60); (e) PHB/PELA (20/80); (f) PELA.

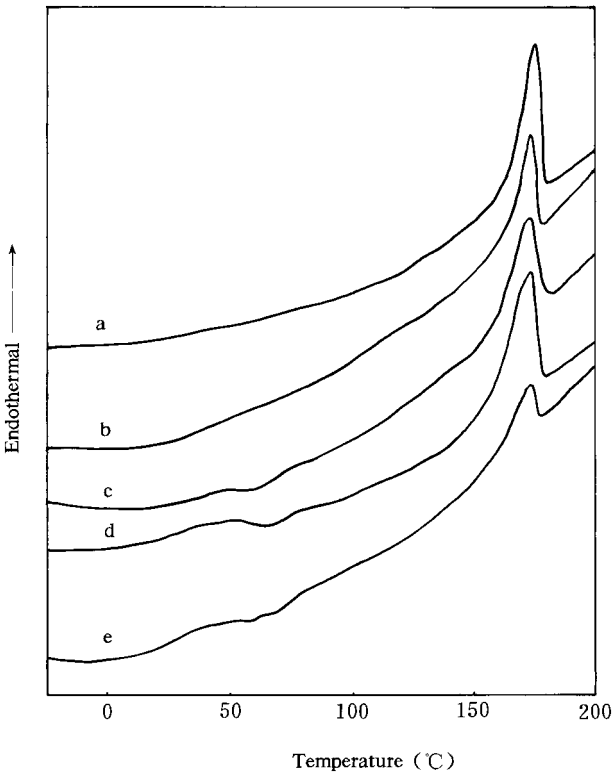

Figure 2 Differential scanning calorimetry (DSC) thermograms of samples after a DSC cooling run at a rate of 20°C/min and during a heating run at a rate of 20°C/min: (a) PHB; (b) PHB/PELA (80/20); (c) PHB/PELA (60/40); (d) PHB/PELA (40/60); (e) PHB/PELA (20/80).

Melting and Cold Crystallization

Samples as cast films were first heated from −60 to 200°C at a heating rate of 20°C/min. The melting temperatures (T_m) and apparent melting enthalpy (ΔH_f) were determined from DSC endothermal peaks. After 1 min samples were cooled to −60°C at a cooling rate of 100°C/min. Finally, the samples were reheated to 200°C at a rate of 20°C/min. The T_m, ΔH_f, temperatures of cold crystallization (T_{cc}), and enthalpy of cold crystallization (ΔH_{cc}) were obtained from this run.

Nonisothermal Crystallization

The samples as cast films were first heated to 200°C at a rate of 20°C/min; after 1 min they were cooled to −60°C at a rate of 20°C/min. The temperatures of crystallization (T_c) and enthalpy of crystallization (ΔH_c) were determined from DSC exothermal peaks. The samples were then scanned at a heating rate of 20°C/min to determine the T_m and ΔH_f again.

The T_m, T_c, and T_{cc} were taken as the peak values of the respective endothermal or exothermal processes in the DSC curves. In the presence of multiple endothermal peaks, the maximum peak temperature was taken as T_m. The glass transition temperature (T_g) was taken as the midpoint of the specific heat increment.

Polarizing Optical Microscopy

A Leitz Wetzlar Ortholux II POL-BK microscope equipped with a hot stage was used to observe the crystallization and growth of spherulites of PHB in the blends. Samples cut from the cast films were first heated to 200°C, then cooled rapidly to the desired temperature, and allowed to crystallize isothermally under crossed polars.

Scanning Electron Microscopy (SEM)

SEM was performed with AMRAY 1000B equipment operated at 15 or 20 kV to examine the phase morphology. The blend films after toluene etching were used for surface observation. The fractured samples were prepared by submerging

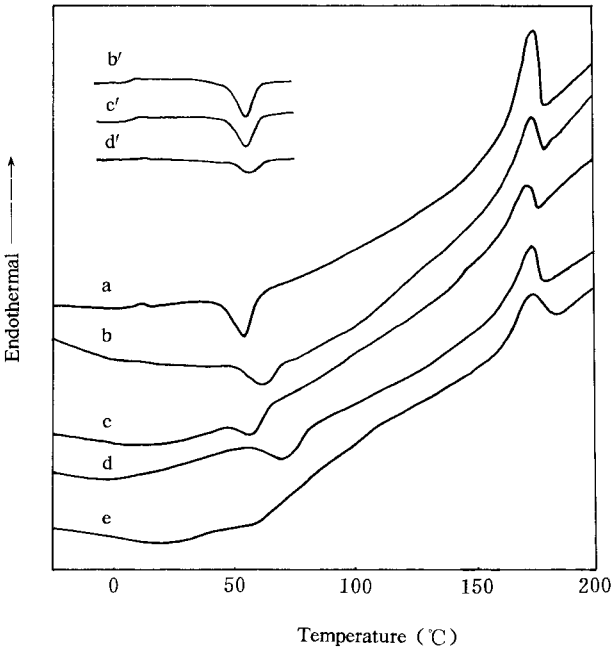

Figure 3 Differential scanning calorimetry (DSC) thermograms of samples after a DSC cooling run at a rate of 100°C/min and during a heating run at a rate of 20°C/min: (a) PHB; (b) PHB/PELA (80/20); (c) PHB/PELA (60/40); (d) PHB/PELA (40/60); (e) PHB/PELA (20/80); (b′) PHB/PDLLA (80/20); (c′) PHB/PDLLA (60/40); (d′) PHB/PDLLA (40/60).

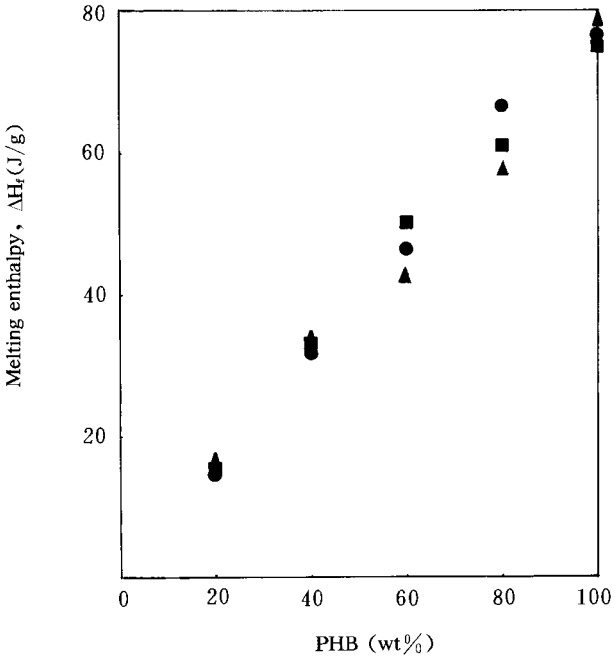

Figure 4 Melting enthalpy of PHB/PELA blends (ΔH_f) as a function of the blend composition: (●) original samples; (■) samples after DSC cooling run at a rate of 20°C/min; (▲) samples after DSC cooling run at a rate of 100°C/min.

cast films in liquid N_2. Before observation, all samples were coated with a thin layer of gold by means of a polaron sputtering apparatus.

RESULTS AND DISCUSSION

Melting Behavior and Blend Morphology

The thermograms of the original samples of the two blend components and the blends during DSC heating runs are shown in Figure 1. PHB and the blends display melting processes with a slight shift in melting temperatures at about 175°C. A glass transition appears at about 31°C in the thermogram of PELA in Figure 1, and the T_g values of PHB/PELA (60/40), (40/60), and (20/80) blends are found at about 30°C. No clear glass transition of PHB or the PHB/PELA (80/20) blend was determined by heating the cast film samples from −60 to 200°C.

After a DSC cooling run at a rate of 20°C/min, similar results were obtained except for exothermal peaks corresponding to cold crystallization of PHB at 60–70°C for PHB/PELA (60/40), (40/60), and (20/80) blends, as shown in Figure 2. For samples after a DSC cooling run at a rate of 100°C/min, PHB showed a glass transition at 8°C; the glass transitions of the blends were found between 10 and 30°C during the DSC heating run (see Fig. 3). However, the T_g values of the blends could not be determined precisely due to the influence of the followed cold crystallization processes of PHB in the blends. In contrast to the immiscible PHB/PDLLA blends with similar thermal history, in which there were no shifts of T_g values for PHB/PDLLA (80/20), (60/40), and (40/60) blends in the corresponding DSC heating run, the PHB/PELA blends were miscible to some extent. Composition-dependent T_g values were also found in the blends containing PHB and PELA with relatively higher PEG contents of 10 and 15 wt %.[33]

The melting enthalpy of the blends, ΔH_f, increased with the increase of PHB content and was close to the value predicted by a linear relation,

$$\Delta H_f = \Delta H_f^{\mathrm{PHB}} \times W^{\mathrm{PHB}} \qquad (1)$$

where ΔH_f and $\Delta H_f^{\mathrm{PHB}}$ are the melting enthalpy

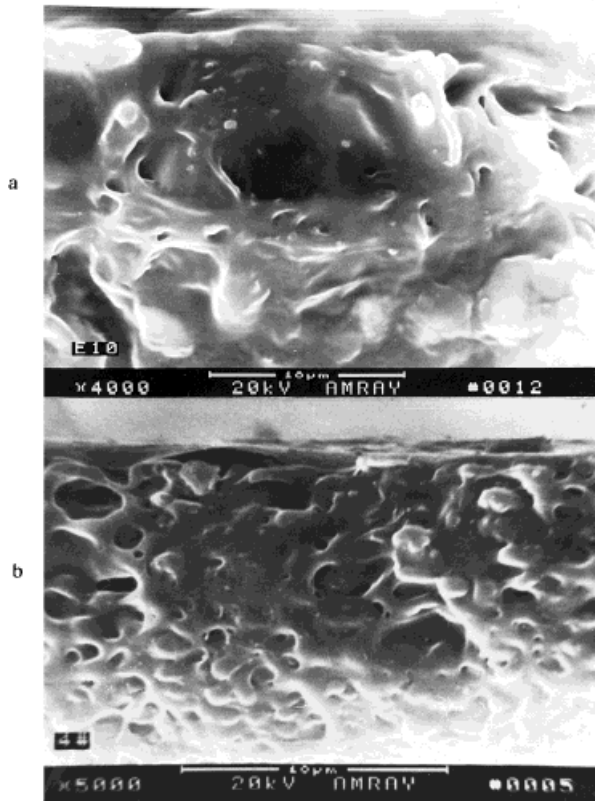

Figure 5 Scanning electron micrographs of the blend films after toluene etching: (a) PHB/PELA (60/40); (b) PHB/PELA (40/60).

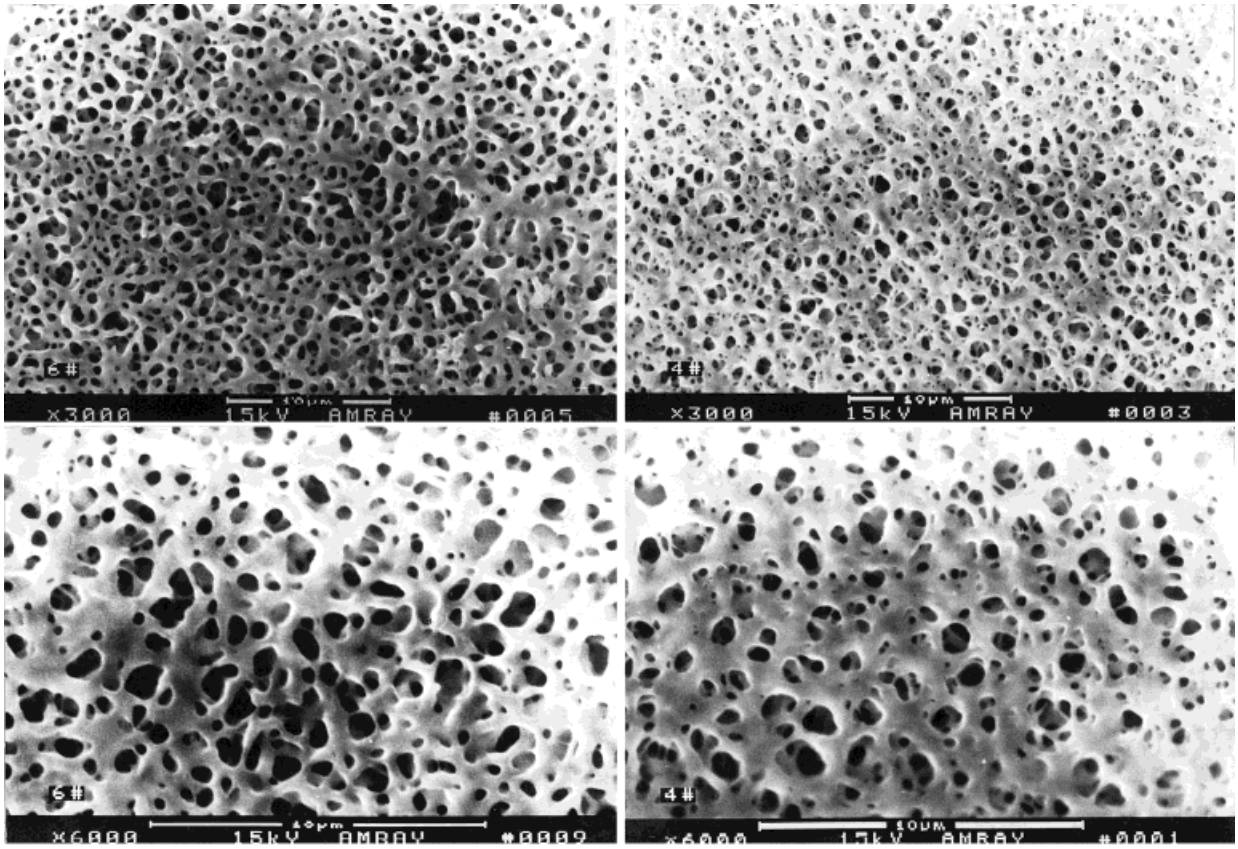

a b

Figure 6 Scanning electron micrographs of the fracture surfaces: (a) PHB; (b) PHB/PELA (40/60).

of the blends and pure PHB, respectively, and W^{PHB} is the weight fraction of the PHB in the blends. The results of ΔH_f are given in Figure 4. The line is drawn according to eq. (1) using the ΔH_f^{PHB} obtained from the first heating run of pure PHB.

SEM photographs of PHB/PELA (60/40) and (40/60) blends taken after toluene etching to remove the PELA phase (Fig. 5) show that the PELA phase is uniformly distributed in the PHB phase. Figure 6 shows the photographs of the fracture surfaces of the PHB and PHB/PELA (40/60) blend. The PHB/PELA (40/60) blend was found to have a smooth texture similar to the pure PHB component.

Crystallization Behavior

During DSC cooling runs at a rate of 20°C/min, exothermal peaks corresponding to the crystallization of PHB were found at about 94, 91, 84, and 82°C for pure PHB, PHB/PELA (80/20), (60/40), and (40/60) blends, respectively (see Fig. 7). No crystallization of PHB was found in the PHB/PELA (20/80) blend. The supercooling temperature, ΔT, was used to describe the kinetic crystallizability during the nonisothermal crystallization process. A higher ΔT indicates lower kinetic crystallizability in the range of T_m to T_g. ΔT is calculated from the T_m and the temperature of nonisothermal crystallization (T_c), $\Delta T = T_m - T_c$. As shown in Table I, the ΔT values of the blends are higher than that of pure PHB, indicating lower kinetic crystallizability of PHB in the blends. On the other hand, the enthalpy of crystallization of the blends (ΔH_c) increases with the increase of PHB content in the blends, as shown in Figure 8. However, the ΔH_c is not much higher than those calculated from the enthalpy of crystallization of pure PHB, $\Delta H_c^{PHB} = 73.5$ J/g, by a linear relation $\Delta H_c = \Delta H_c^{PHB} \times W^{PHB}$ for PHB/PELA (80/20) and (40/60) blends (see Table I).

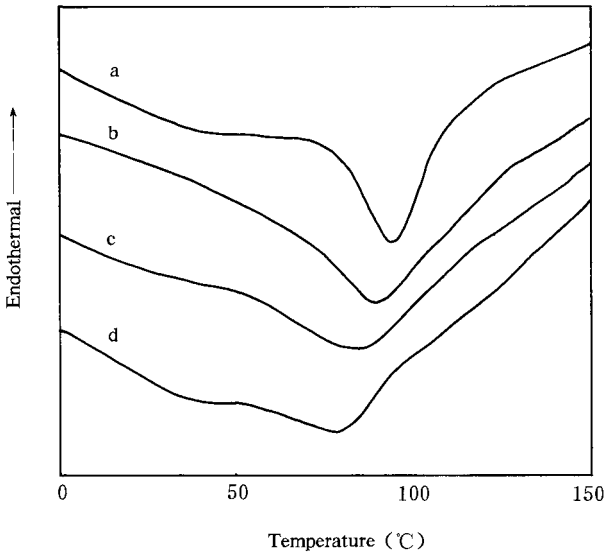

Figure 7 Differential scanning calorimetry curves during a cooling run at a rate of 20°C/min: (a) PHB; (b) PHB/PELA (80/20); (c) PHB/PELA (60/40); (d) PHB/PELA (40/60).

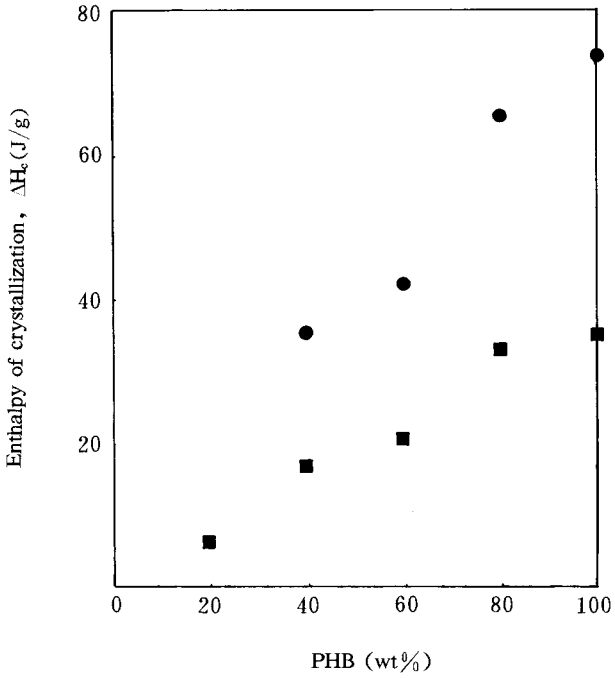

Figure 8 Enthalpy of crystallization as a function of the blend composition: (●) ΔH_c from a DSC cooling run at a rate of 20°C/min; (■) ΔH_{cc}, from a DSC heating run after rapid cooling from the melt at a rate of 100°C/min.

The crystallization of PHB from the melt was also observed using polarizing optical microscopy under isothermal condition. From Figure 9 it is found that well-defined spherulites are present at 80°C for pure PHB and PHB/PELA (80/20) and (60/40) blends. In the PHB/PELA (40/60) blend PHB can also crystallize according to a spherulitic morphology, but the growth of a spherulite of PHB is affected by the PELA component.

When cooled from the melt at a rate of 100°C/min, only pure PHB crystallized incompletely at a T_c of about 73°C with a much lower enthalpy of crystallization than that from the DSC cooling run at a rate of 20°C/min. The rapidly cooled samples were then heated to 200°C, and exothermal peaks corresponding to the cold crystallization of PHB appeared in the DSC curves as shown in Figure 3. The cold crystallization of PHB was also affected by the PELA component. The exothermal peaks shifted to higher temperatures, and the enthalpy of cold crystallization of the blends, ΔH_{cc}, decreased with the increase of PELA content in the blends, as shown in Figure 8. Because pure PHB and PHB in the PHB/PELA (80/20) blend can completely crystallize during a DSC cooling

Table I Temperature and Enthalpy of Nonisothermal Crystallization (T_c, ΔH_c) from Melt at 20°C/min

Sample Code	T_m[a] (°C)	T_c[b] (°C)	ΔT[c] (°C)	ΔH_c[b] (J/g)	ΔH_c[d] (J/g)
PHB	176	94.2	81.8	73.5	73.5
PHB/PELA (80/20	174	91.3	82.7	65.5	58.8
PHB/PELA (60/40)	174	84.3	89.7	42.1	44.1
PHB/PELA (40/60)	175	82.0	93.0	35.6	29.4

[a] Obtained from the first heating run of the original samples.
[b] Determined from the exothermal peaks during the DSC cooling run.
[c] Calculated from the relation $\Delta T = T_m - T_c$.
[d] Calculated from the relation $\Delta H_c = \Delta H_c^{PHB} \times W^{PHB}$. ΔH_c^{PHB} is the enthalpy of crystallization of pure PHB: $\Delta H_c^{PHB} = 73.5$ J/g.

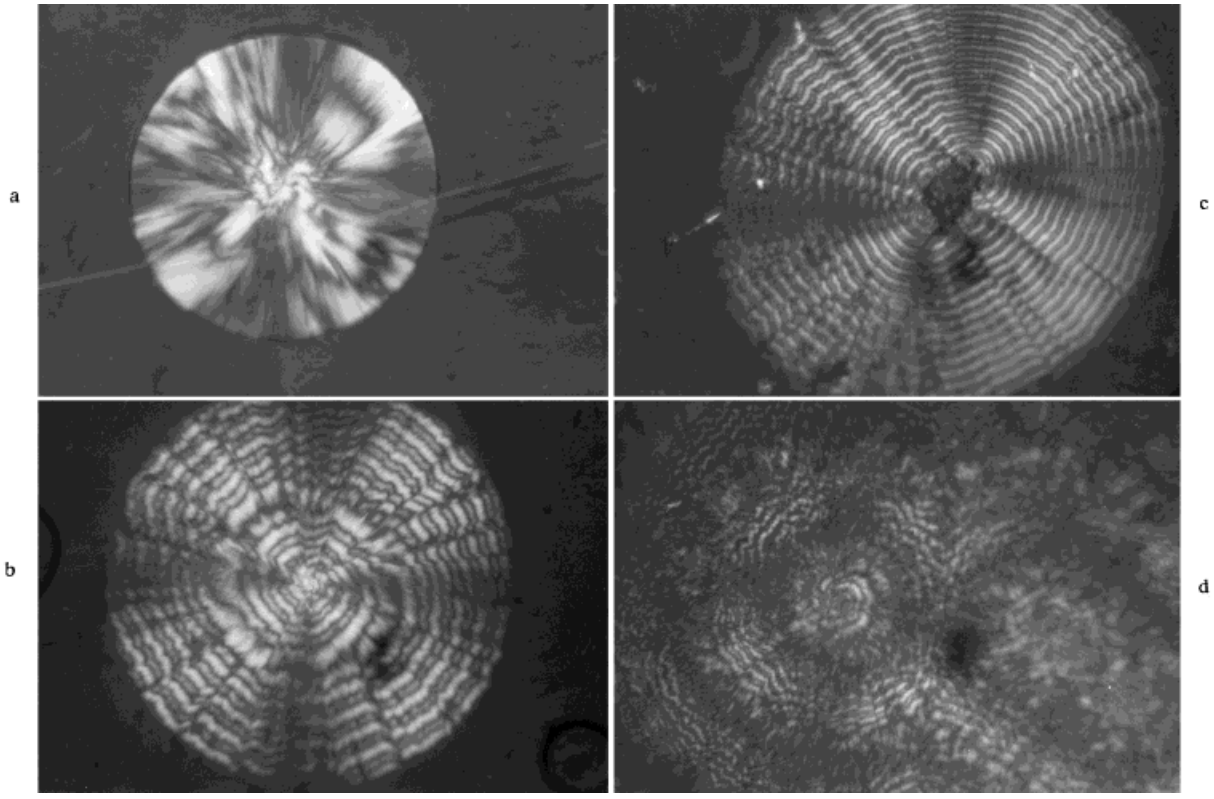

Figure 9 Polarizing optical micrographs of PHB and PHB/PELA blends under crossed polars (same magnification, bar = 0.1 mm): (a) PHB; (b) PHB/PELA (80/20); (c) PHB/PELA (60/40); (d) PHB/PELA (40/60).

run at a rate of 20°C/min, no glass transition and cold crystallization are present at the followed heating run (see Fig. 2). However, exothermal peaks of cold crystallization of PHB were found for PHB/PELA (60/40), (40/60), and (20/80) blends. The T_{cc} values of PHB in the blends in Figure 2 are higher than that of pure PHB in Figure 3. The ΔH_{cc} of the blend after the cooling run at a rate of 20°C/min was much lower than that of the corresponding samples after the cooling run at a rate of 100°C/min.

CONCLUSIONS

The T_g of PHB/PELA (60/40), (40/60), and (20/80) blends was about 30°C, which was close to that of pure PELA obtained during DSC heating runs of the original samples. Similar results were found for samples after a DSC cooling run at a rate of 20°C/min. After cooling at a rate of 100°C/min, PHB showed a glass transition at 8°C; the T_g values of the blends were found between 10 and 30°C. The results confirmed that PHB/PELA blends were miscible to a certain extent. The melting enthalpy of the blends increased with the increase of PHB content in the blends and was close to that predicted by a linear relationship. As shown by SEM, two phases were distributed uniformly in the blends. The kinetic crystallizability of PHB in the blends decreased with an increase of PELA content. Well-defined spherulites of PHB were found in pure PHB and PHB/PELA (80/20) and (60/40) blends. Cold crystallization of PHB was also affected by the PELA component with cold crystallization peaks shifted to higher temperatures.

The authors are grateful to the National Natural Science Foundation of China, the Postdoctoral Science Foundation of China, and the National Key Laboratory of Engineering Plastics, Institute of Chemistry, Academia Sinica, for financial support of this work.

REFERENCES

1. P. A. Holmes, *Phys. Technol.,* **16,** 32 (1985).
2. Y. Doi, *Microbial Polyesters,* VCH Publishers, New York, 1990.

3. P. J. Barham and A. Keller, *J. Polym. Sci., Polym. Phys. Ed.,* **24,** 69 (1986).
4. P. J. Hocking and R. H. Marchessault, in *Chemistry and Technology of Biodegradable Polymers,* G. J. L. Griffin, Ed., Chapman & Hall, London, 1994, p. 48.
5. Y. Doi, *Macromol. Chem. Phys. Macromol. Symp.,* **98,** 585 (1995).
6. M. Avella and E. Martuscelli, *Polymer,* **29,** 1731 (1988).
7. M. Avella, E. Martuscelli, and P. Greco, *Polymer,* **32,** 1647 (1991).
8. M. Avella, E. Martuscelli, and M. Raimo, *Polymer,* **34,** 3234 (1993).
9. J. S. Yoon, C. S. Choi, S. J. Maing, H. J. Choi, H.-S. Lee, and S. J. Choi, *Eur. Polym. J.,* **29,** 1359 (1993).
10. H. J. Choi, S. H. Park, J. S. Yoon, H.-S. Lee, and S. J. Choi, *Polym. Eng. Sci.,* **35,** 1636 (1995).
11. H. Marand and M. Collins, *ACS Polym. Prepr.,* **31,** 552 (1990).
12. S. L. Edie and H. Marand, *ACS Polym. Prepr.,* **32,** 329 (1991).
13. P. Greco and E. Martuscelli, *Polymer,* **30,** 1475 (1989).
14. M. Abbate, E. Martuscelli, G. Ragosta, and G. Scarinzi, *J. Mater. Sci.,* **26,** 1119 (1991).
15. E. Dubini Paglia, P. L. Beltrame, M. Canetti, A. Seves, B. Marcandalli, and E. Martuscelli, *Polymer,* **34,** 996 (1993).
16. P. Sadocco, M. Canetti, A. Seves, and E. Martuscelli, *Polymer,* **34,** 3368 (1993).
17. P. Sadocco, C. Bulli, G. Elegir, A. Seves, and E. Martuscelli, *Macromol. Chem.,* **194,** 2675 (1993).
18. Y. Azuma, N. Yoshie, M. Sakurai, Y. Inoue, and R. Chûjô, *Polymer,* **33,** 4763 (1992).
19. N. Yoshie, Y. Azuma, M. Sakurai, and Y. Inoue, *J. Appl. Polym. Sci.,* **56,** 17 (1995).
20. P. Iriondo, J. J. Iruin, and M. J. Fernandez Berridi, *Polymer,* **36,** 3235 (1995).
21. N. Lotti, M. Pizzoli, G. Ceccorulli, and M. Scandola, *Polymer,* **34,** 4935 (1993).
22. M. Canetti, P. Sodocco, A. Siciliano, and A. Seves, *Polymer,* **35,** 2384 (1994).
23. A. Siciliano, A. Seves, T. De Marco, S. Cimmino, E. Martuscelli, and C. Silvestre, *Macromolecules,* **28,** 8065 (1995).
24. E. Blümm and A. J. Owen, *Polymer,* **36,** 4077 (1995).
25. L. L. Zhang, C. D. Xiong, and X. M. Deng, *Polymer,* **37,** 235 (1996).
26. F. Gassner and A. J. Owen, *Polymer,* **35,** 2233 (1994).
27. A. Lisuardi, A. Schoenberg, M. Gada, R. A. Gross, and S. P. McCarthy, *Polym. Mater. Sci. Eng.,* **67,** 298 (1992).
28. L. L. Zhang and X. M. Deng, *Polym. Mater. Sci. Eng.* [in Chinese], **10,** 64 (1994).
29. H. Abe, Y. Doi, and Y. Kumagai, *Macromolecules,* **27,** 6012 (1994).
30. R. Pearce, J. Jesudason, W. Orts, R. H. Marchessault, and S. Bloembergen, *Polymer,* **33,** 4647 (1992).
31. R. Pearce, G. R. Brown, and R. H. Marchessault, *Polymer,* **35,** 3984 (1994).
32. R. Pearce and R. H. Marchessault, *Polymer,* **35,** 3990 (1994).
33. L. L. Zhang, C. D. Xiong, and X. M. Deng, *J. Appl. Polym. Sci.,* **56,** 103 (1995).
34. S. J. Zhao, C. Y. Fan, X. Hu, J. R. Chen, and H. F. Feng, *Appl. Biochem. Biotechnol.,* **39/40,** 191 (1993).
35. S. Akita, Y. Einaga, Y. Miyaki, and H. Fujita, *Macromolecules,* **9,** 774 (1976).
36. X. M. Deng, C. D. Xiong, L. M. Cheng, and R. P. Xu, *J. Appl. Polym. Sci.,* **56,** 1193 (1995).